Selection of $B_s^0 \to \psi(2S)K_S^0$ decays via multivariate analysis

Lukas Bertsch
lukas.bertsch@tu-dortmund.de

Tabea Hacheney
tabea.hacheney@tu-dortmund.de

Tom Troska
tom.troska@tu-dortmund.de

Start of course: 13th of June 2024

TU Dortmund University – Faculty of Physics

Contents

1. Theorie

[1]

2. The LHCb detector

Located at CERN, the LHC is the largest particle collider in the world and houses a number of experiments. Protons are collided at a center-of-mass energy of 999 TeV at four different interaction points. At one of these, the LHCb experiment is installed. This detector is constructed as a single-arm forward spectrometer with allows for an optimized detection in the pseudorapidity range of $2 \leq \eta \leq 5$. With the help of this design, the LHCb detector is well suited for the detection of decays that include b and c quarks because the production of these is favored for small angles along the beam axis.
The LHCb experiment consists of serveral sub-detectors, each with a different special purpose. A cross-section of the detector used during the second data-taking run is depicted in Figure 1. In the immediate proximity of the interaction point, the Vertex

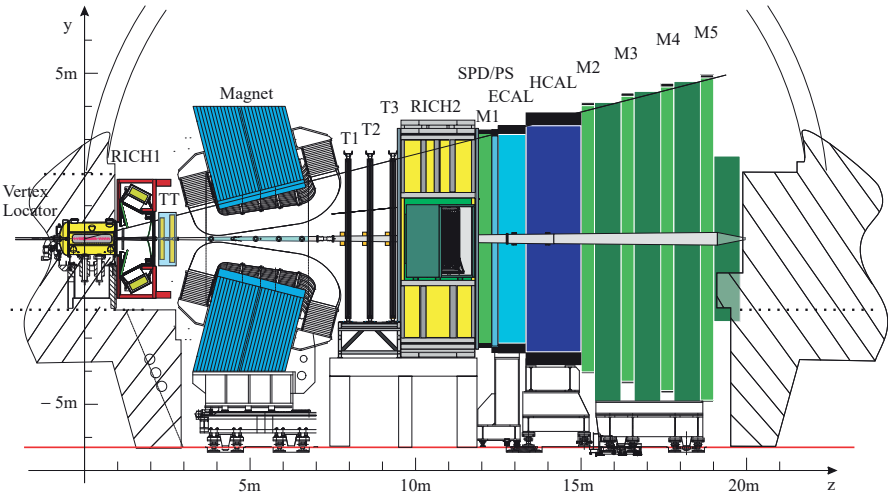

Figure 1: Cross-section of the LHCb detector. A right-handed coordinate system with the z-axis parallel to the beam pipe and the y-axis orientated to the top is used to describe the detector.The different sub-detectors and their purpose and functionality are discussed in this section [2].

Locator (VELO) is located. Primary and secondary vertices are identified by the 52 silicon pixel modules. The detector is divided into two halves that are retractable. During the injection phase, the VELO is sitting in its retracted position because the beam is not as focused as during the stable beam phase. Due to the closeness of the VELO to the interaction point, the primary veritices can be reconstructed with great accuracy.
One of the two Ring Imaging Cherenkov detectors (RICH) is located right before the 1.4 T dipole magnet while the other RICH detector is situated behind the tracking stations. Two materials with different refractive indices are used in the two RICH detectors to

determine the velolcity of the particles via the Cherenkov effect. The implementation of two detectors allows for a larger momentum range reconstruction.
The position of the particles are detected by the tracking stations, the Tracker Turicensis (TT) and T1-T2. With this information and the previously measured velolcity, the momentum of the particles can be calculated.
For the determination of the energy of the particles, the electromagnetic and hadronic calorimeters (ECAL and HCAL) are employed. To accomplish this task for the ECAL, the shashlik calorimeter technology is used. Here, an absorber material and a detector layer of a scintillating material are stacked alternately. The HCAL is constructed similarly but with the scintillating tiles running parallel to the beam axis.
Muon stations at the end of the detector identify the muons that are passing through the detector. This is accomplished by four multi-wire proportional chambers.
Because of the large number of potential events, a trigger system is used to identify interesting decays. The data of these are then saved for further offline analysis.

3. Auswertung

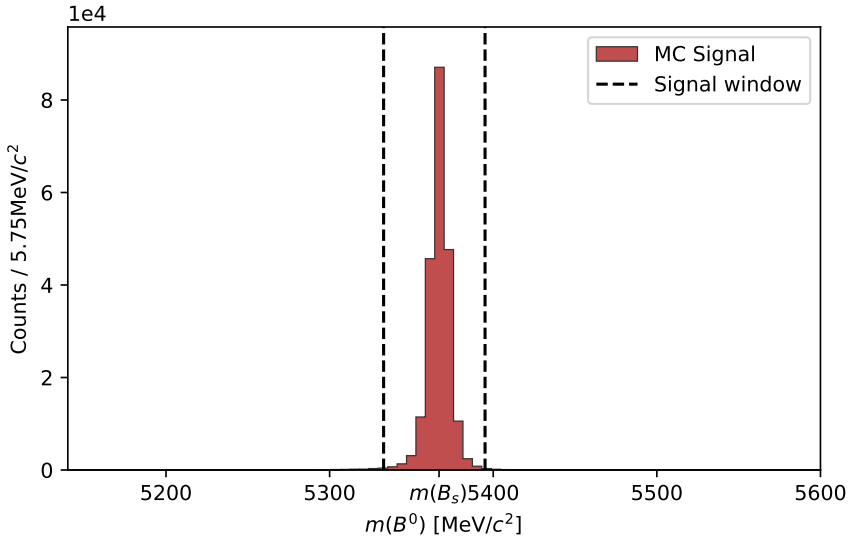

Figure 2: Invariant mass distribution of the B_s^0 candidates for the signal channel simulation data.

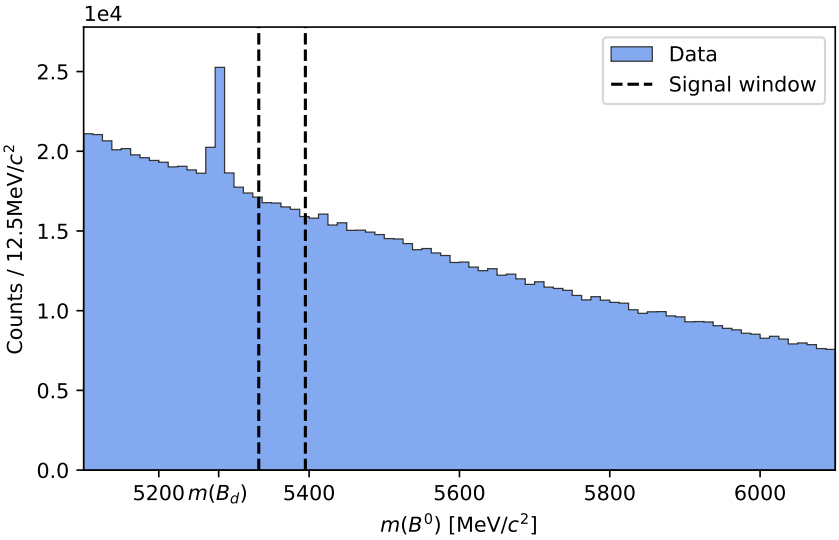

Figure 3: Invariant mass distribution of the B^0 candidates for the recorded LHCb data.

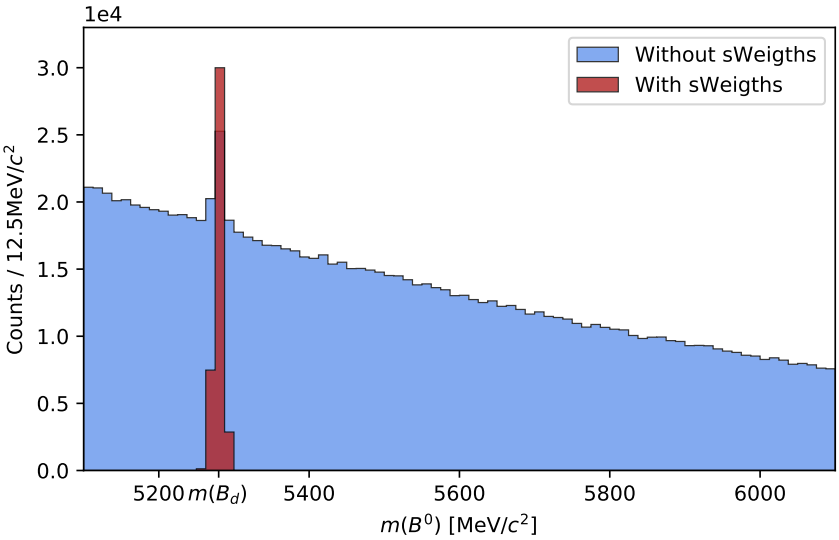

Figure 4: Invariant mass distribution of the B^0 candidates for the recorded LHCb data and sWeights reweighted data.

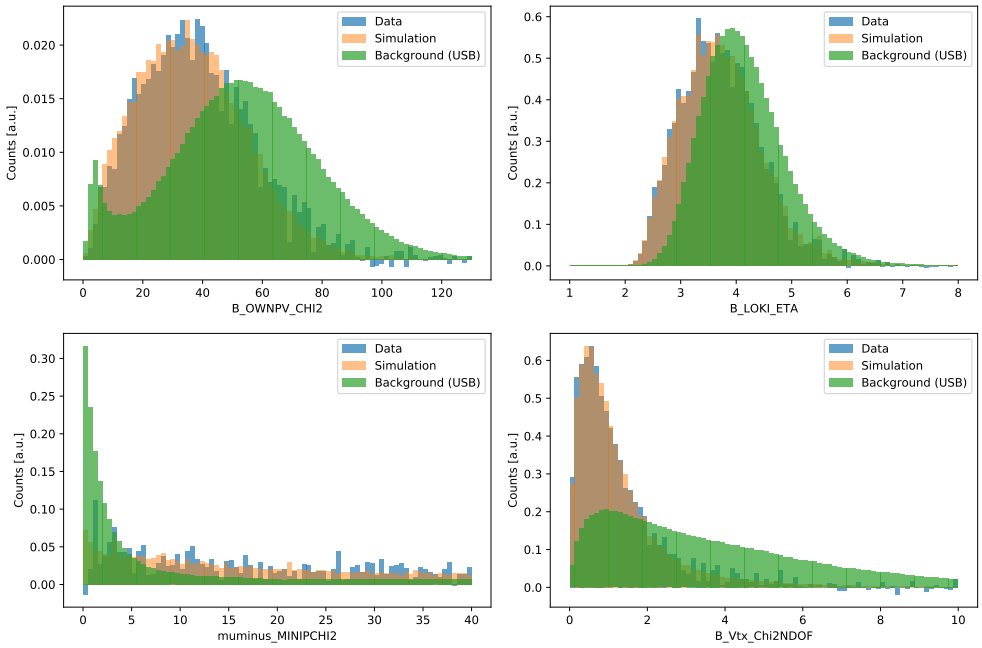

Figure 5: Distributions of four selected variables used in the MVA for simulation, reweighted data and background.

3.1. Feature selection

3.2. Training of MVA classifier

3.3. Optimization of the classification threshold

3.4. Evaluation of the signal yield

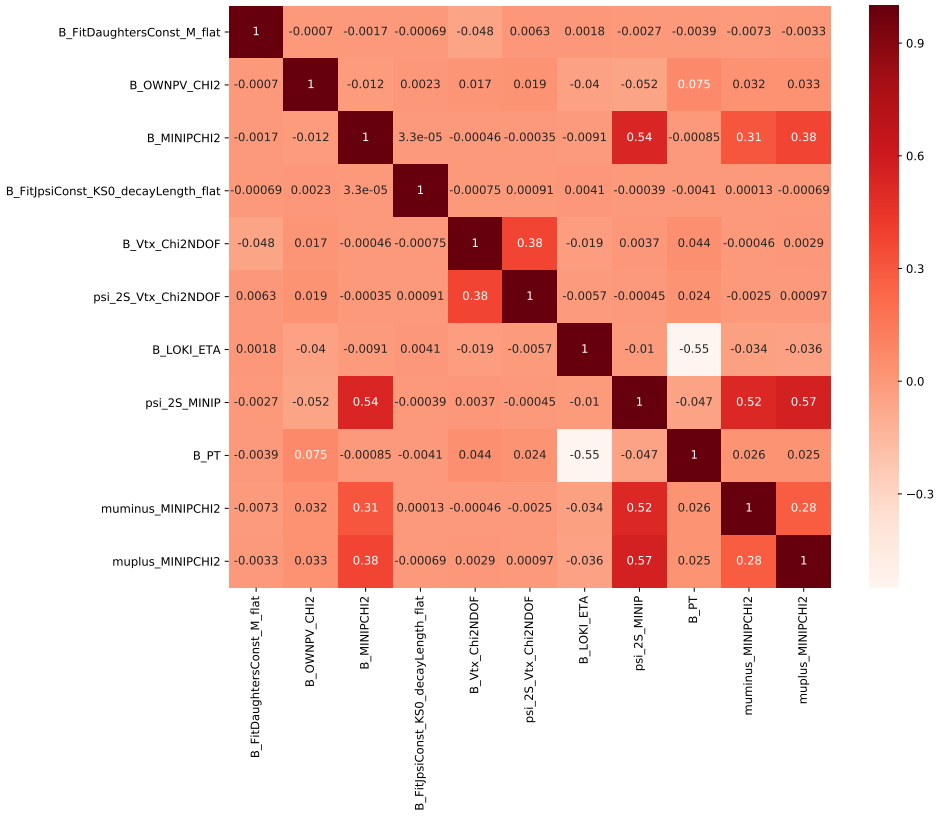

Figure 6: Correlations between the 10 selected variables and the reconstructed B^0 mass.

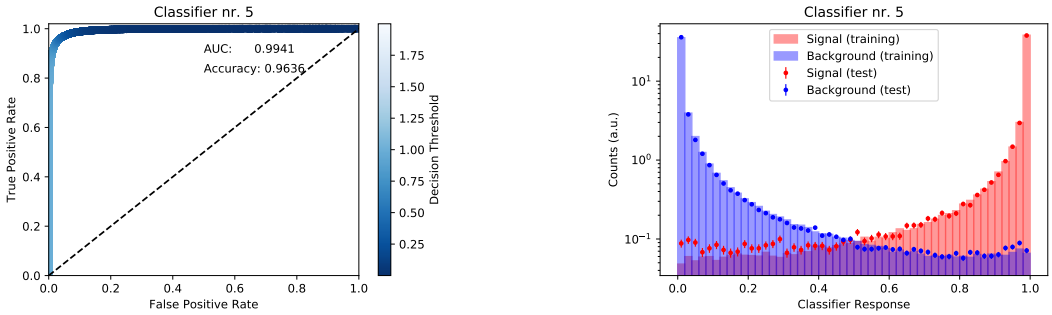

Figure 7: ROC curve (left) and performance on training and test dataset for one of the trained classifiers.

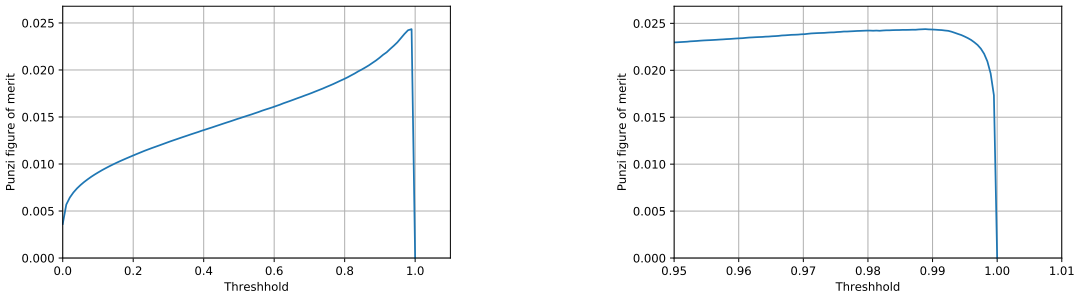

Figure 8: The Punzi figure of merit for the mean classifier response in different intervals of the threshold.

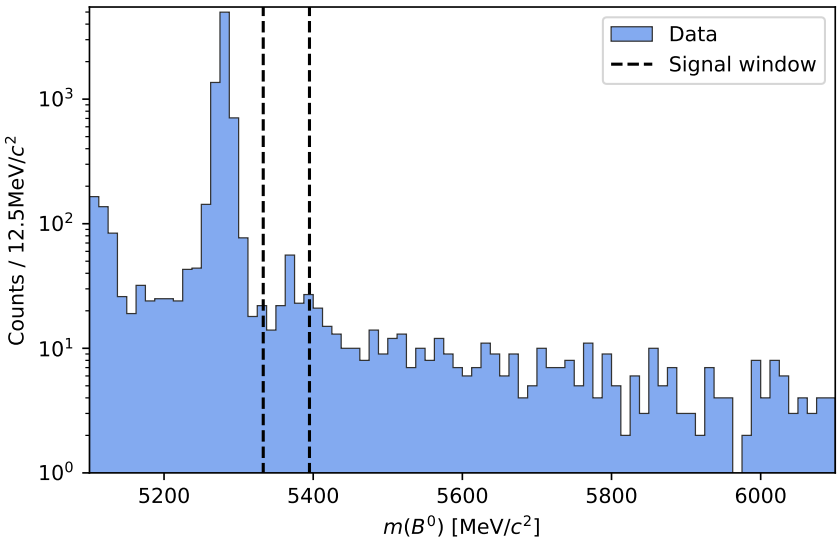

Figure 9: Semi logarithmic invariant mass distribution of the B^0 candidates in data, after the cut on the classifier response is applied.

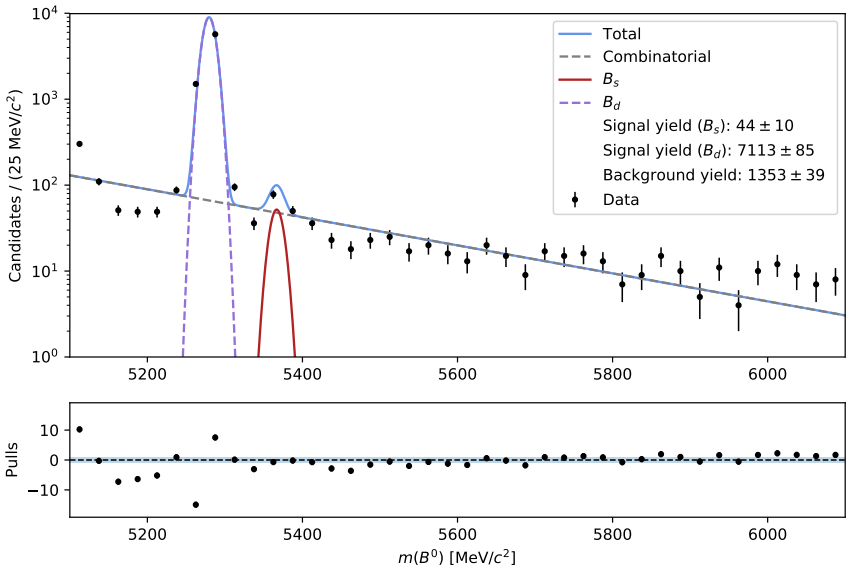

Figure 10: Fit to the invariant mass spectrum of the data in semi logarithmic depiction.

4. Diskussion

References

[1] *Versuch zum Literaturverzeichnis*. TU Dortmund, Fakultät Physik. 2022.

[2] A. Augusto Alves Jr. et al. 'The LHCb Detector at the LHC'. In: *JINST* 3 (2008), S08005. DOI: 10.1088/1748-0221/3/08/S08005.

A. Anhang

A.1. Originaldaten